
‘Si’multaneous ‘S’patial-‘T’emporal Message Passing for Dynamic Graph Representation Learning

Shubhajit Roy

Department of Computer Science and Engineering
Indian Institute of Technology Gandhinagar

royshubhajit@iitgn.ac.in

Anirban Dasgupta

Department of Computer Science and Engineering
Indian Institute of Technology Gandhinagar

anirbandg@iitgn.ac.in

Abstract

Dynamic graph neural networks (DGNNs) that operate on snapshot sequences typically fall into one of two categories. *Temporal-first* approaches build per-node temporal embeddings and only afterwards perform spatial aggregation, whereas *Spatial-first* approaches invert this order, feeding the output of a graph convolution into a downstream temporal module. In either case, the rigid sequencing forces the second stage to consume an already-compressed summary produced by the first, ruling out joint reasoning over topology and evolution; concretely, the message-passing operator never gets to weight a neighbor’s contribution by that neighbor’s *past* trajectory. This paper introduces **SiST-GNN** (**Simultaneous Spatial-Temporal GNN**), which fuses the two signals inside a single message-passing operation rather than chaining them. Concretely, at each snapshot we maintain a recurrent hidden state per node that summarises its history, pair it with the node’s current feature vector, and treat the pair as two nodes joined by a cross-time edge; running a standard graph convolution on this temporally augmented graph yields the updated representation. Our empirical study spans nine public baselines and fourteen model-dataset combinations, covering both fixed-split and live-update evaluation regimes. Across every public benchmark, SiST-GNN sets a new state of the art in link prediction task over the strongest prior method by 109–277% in the fixed-split setting and by 68–194% in the live-update setting. We additionally construct three dynamic node-classification tasks by discretising the underlying continuous-time event streams; here SiST-GNN beats the leading discrete-time (DTDG) baseline by 7–22% and matches continuous-time (CTDG) methods that consume the raw events directly.

1 Introduction

Most consequential relation systems, such as financial transaction networks, peer-to-peer trust graphs, and communication in social platforms, are inherently *dynamic*: their topology and node attributes co-evolve over time Kazemi et al. (2020); You et al. (2022). Forecasting the next interaction in such a system is a canonical *Dynamic Link Prediction* problem, and it has been tackled by a variety of DGNNs Pareja et al. (2020); da Xu et al. (2020); Rossi et al. (2020); Sankar et al. (2020); Trivedi et al. (2019); Yu et al. (2023). In an analogous setting, a subset of nodes may exhibit anomalous behavior. Consequently, detecting these anomalies is formulated as a *node classification* task within the graph. DGNNs Leskovec et al. (2005); Rossi et al. (2020); Trivedi et al. (2019); Wang et al. (2021b); Seo et al. (2018) are frequently employed to address this challenge.

When the input is discretized into a sequence of snapshots $\{\mathcal{G}_1, \dots, \mathcal{G}_T\}$ as is standard for trust networks, citation streams, and routing data, existing DGNNs almost universally adopt one of two architectural paradigms.

- **Temporal-First (T→S):** A recurrent or attention-based module first encodes the node feature *trajectory*, and the resulting temporal summary is then passed to a GNN. Representative examples include EvolveGCN Pareja et al. (2020), where an RNN evolves the GNN’s *weights*.
- **Spatial-first (S→T):** A GNN is applied per snapshot, and the resulting structural embeddings are further processed by a temporal module such as a GRU or LSTM. This is the dominant pattern, instantiated by GCRN Seo et al. (2018), T-GCN Zhao et al. (2020), ROLAND You et al. (2022) and TMetaNet Li et al. (2025).

The Information bottleneck. What both paradigms share is a strict *ordering*. One modality is consumed in full before the other is allowed to look at it. The downstream module can therefore only influence the final representation via the transformed output of the upstream module, and, crucially, it cannot modulate which information the upstream module retains. A spatial-first model, for example, cannot let its message-passing operator condition the aggregation of a node v ’s feature on v ’s historical activity, because no temporal information has been computed yet. Simultaneously, a temporal-first model cannot let its recurrent cell condition on the current structural neighborhood. We argue that this rigidity is responsible for a substantial part of the gap between current DGNNs.

Simultaneous fusion as a third paradigm. We propose that the two signals should interact within a single message-passing step. For every node v , we maintain a recurrent hidden state $\mathbf{h}_v^{(t)}$ that summarizes its trajectory, and at every snapshot we build a *temporally augmented graph* with N additional vertices, where the first N carry the current spatial features $\text{proj}(\mathbf{X}_t)$, and the next N carry the recurrent summaries $\tilde{\mathbf{X}}_t$. For every original edge $(u, v) \in \mathcal{E}_t$ we add a cross-time edge $(u + N, v)$ and $(u + N, u)$, so that each node receives both the present-time feature and the temporal summary of every neighbor and itself, all within one graph convolution. The output of the first N vertices is the next-layer representation.

This simple construction has two consequences: first, the GNN operates on a richer message pool where each node sees $|\mathcal{N}(u)|$ structural messages *and* $|\mathcal{N}(u)| + 1$ temporal messages per layer, with the feature sets distinguishable by the message-passing operator through a standard aggregation function. Second, the assignment between spatial and temporal information becomes *data-dependent and paper-neighbor*: a node can attend more to a neighbor’s recent history when its current features are uninformative, and conversely fall back on present structure when temporal context is stale.

Contributions. We make the following contributions:

- We identify an architectural bottleneck shared by all snapshot based DGNNs that imposes ordering between spatial and temporal computation, and motivate *simultaneous* spatial-temporal message passing as a third paradigm (Section 4).
- We instantiate this paradigm as **SiST-GNN**: a stackable layer that fuses a recurrent cell with a graph convolution over a temporally augmented graph (Section 4).
- We evaluate SiST-GNN against eight baselines, spanning static GNNs, snapshot DGNNs, evolving-weight architectures, ROLAND variants, and the meta-learner TMetaNet Li et al. (2025), on six public benchmarks under fixed-split *and* live-update protocols. SiST-GNN attains the best MRR on *every* dataset and setting, improving over the baseline by 109 – 277% (fixed-split) and 68 – 194% (live-update).
- We further demonstrate that the same architecture on *dynamic node classification*, discretizing the continuous-time datasets with event streams, into fixed-width snapshots, SiST-GNN improves test AUC by 7 – 22% over the discrete-time baseline *and achieves comparable results to continuous-time models*, which operate on the native event stream (Section 5.5).

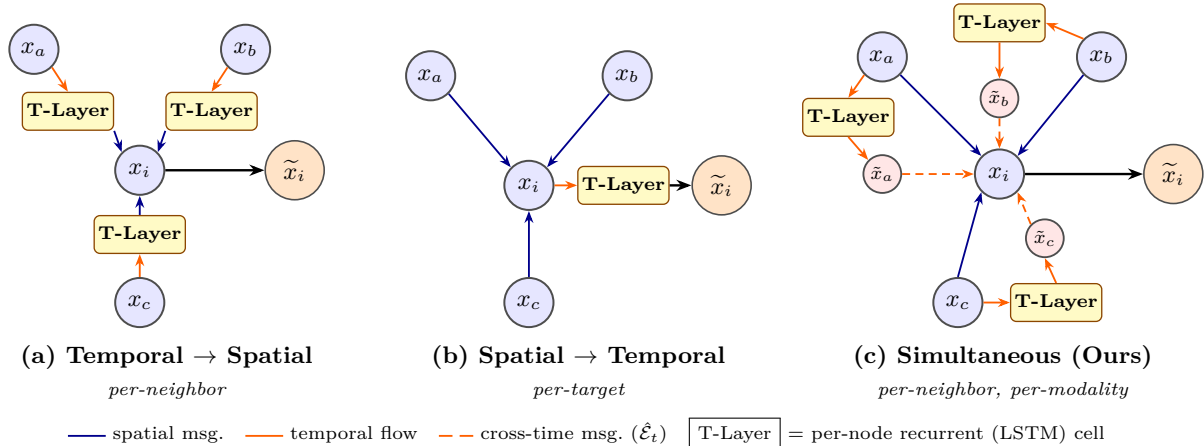


Figure 1: Three paradigms for snapshot-based dynamic GNNs, viewed at the per-target node x_i with neighbors $\{x_a, x_b, x_c\}$. (a) *Temporal-first* encodes each neighbor’s feature trajectory through a temporal layer and *then* aggregates the temporal summaries spatially. (b) *Spatial-first* aggregates neighbor features spatially into x_i and *then* applies a temporal layer to the aggregated representation. (c) Our *simultaneous* paradigm maintains, for every node, a temporal counterpart \tilde{x}_v produced by a per-node T-Layer; the original neighbor features *and* their temporal counterparts both reach x_i within a *single* graph convolution over the temporally augmented graph $\hat{\mathcal{G}}_t$, via solid intra-time edges and dashed cross-time edges. The message-passing operator can therefore learn a per-neighbor, per-modality trade-off between present structure and historical evolution.

2 Related Work

Static graph neural networks. Modern graph representation learning is built on the family of message-passing networks initiated by GCN Kipf & Welling (2017), GraphSAGE Hamilton et al. (2017), GAT Veličković et al. (2018), and GIN Xu et al. (2019). SiST-GNN is agnostic to the underlying spatial operator, hence any of these layers can be plugged into the augmented-graph convolution.

Continuous-time DGNNs. A first family of DGNN models the graph as a stream of timestamped events. TGN Rossi et al. (2020), TGAT da Xu et al. (2020), JODIE Kumar et al. (2019), DyRep Trivedi et al. (2019), CAW Wang et al. (2021c), and APAN Wang et al. (2021b) update node memories at every event using time-aware attention or recurrence, and have produced impressive results on fine-grained interaction data. Continuous-time approaches require per-edge temporal encodings and are less natural when the data is intrinsically snapshot-structured Poursafaei et al. (2022); Huang et al. (2023); Cong et al. (2023). A recent survey Feng et al. (2026) provides a unified benchmark of CTDG and DTDG methods across link prediction and node classification.

Snapshot-based DGNNs: temporal-first. EvolveGCN-H and Evolv-eGCN-O Pareja et al. (2020) treat dynamic graph learning as a meta-learning problem over GNN *weights*: an RNN evolves the GCN parameters across snapshots, while the per-snapshot graph convolution remains static. WinGNN Zhu et al. (2023) drops explicit temporal encodings altogether and instead aggregates stochastic gradients across a sliding window of snapshots.¹

Snapshot-based DGNNs: spatial-first. GCRN Seo et al. (2018) and T-GCN Zhao et al. (2020) first apply spectral or spatial convolutions and then aggregate the embeddings with a GRU or LSTM. DySAT Sankar et al. (2020) replaces the recurrence with self-attention over snapshot embeddings. ROLAND You et al. (2022) generalizes the pattern, observing that any static GNN can be “dynamized” by recurrently updating

¹We were unable to reproduce the WinGNN MRR results. We therefore omit WinGNN from our results tables and treat it as related work.

its hierarchical node states between snapshots, and introduces both a scalable incremental-training procedure and a live-update evaluation protocol that we adopt. DyGFormer Yu et al. (2023) and decoupled architectures Zheng et al. (2023) further refine this template with neighbor co-occurrence features and decoupled propagation. TMetaNet Li et al. (2025) augments the spatial-first pipeline with Dowker zigzag persistence diagrams that guide a meta-learning parameter-update rule. Like all spatial-first models, TMetaNet computes a per-snapshot structural embedding before any temporal signal has interacted with the message passing.

Other related ideas. Variational dynamic embeddings Hajiramezanali et al. (2019); Goyal et al. (2020; 2018); Nguyen et al. (2018) and meta-learning-based dynamic models Zhu et al. (2023); Li et al. (2025) share with us the high-level goal of better leveraging temporal context, but all operate within the sequential paradigm. Our construction of an augmented edge set bears a superficial resemblance to heterogeneous graph design Wang et al. (2021a), where multiple semantic edge types are introduced by domain knowledge, but ours is that cross-time edges are added deterministically from the existing edge set without external annotation.

Dynamic node classification. A complementary line of work targets *dynamic node classification* on the JODIE benchmarks Kumar et al. (2019), which are released as continuous-time event streams. Continuous-time models such as TGAT da Xu et al. (2020) and TGN Rossi et al. (2020) consume these streams directly, while TREND Wen & Fang (2022) and GraphMixer Cong et al. (2023) target the same setting through Hawkes-process and MLP-mixer formulations, respectively. More recently, prompt-based pre-training methods Yu et al. (2025) learn a shared encoder upstream and adapt it to downstream tasks through node- and time-conditional prompts. Our work is orthogonal to this pre-training direction: we treat the task as supervised snapshot-based classification and do not pre-train on auxiliary objectives. We discuss this gap in Section 6.

Positioning of this work. To the best of our knowledge, SiST-GNN is the first snapshot-based DGNN in which the per-node temporal state and the spatial neighborhood enter the *same* graph convolution as neighbors, with separable but jointly-trained aggregation weights. The closest design philosophy is the two-stream decoupled GNN of Zheng et al. (2023), but that work still combines the streams by late-stage concatenation rather than by a single joint message-passing step.

3 Preliminaries and Problem Formulation

Definition 3.1 (Dynamic graph sequence). *A dynamic graph sequence is an ordered collection $\{\mathcal{G}_t = (\mathcal{V}_t, \mathcal{E}_t, \mathbf{X}_t)\}_{t=1}^T$, where \mathcal{V}_t is the node set at snapshot t (with $|\mathcal{V}_t| = N$), $\mathcal{E}_t \subseteq \mathcal{V}_t \times \mathcal{V}_t$ is the edge set, and $\mathbf{X}_t \in \mathbb{R}^{N \times d}$ encodes node features at t .*

We work with the standard ROLAND You et al. (2022) setting, in which nodes are indexed consistently across time, where a node absent in snapshot t has no incident edges in \mathcal{E}_t but retains its identifier.

For *future link prediction* experiments: given $\{\mathcal{G}_1, \dots, \mathcal{G}_t\}$, predict the probability of an edge $(u, v) \in \mathcal{V} \times \mathcal{V}$ being present in \mathcal{G}_{t+1} .

For *node classification* of anomalous nodes: $\{\mathcal{G}_1, \dots, \mathcal{G}_t\}$, predict the probability of a node being anomalous in \mathcal{G}_{t+1} .

Definition 3.2 (Temporal-first paradigm). *Given snapshot features \mathbf{X}_t and previous state \mathbf{H}_{t-1} , the temporal-first paradigm computes*

$$\mathbf{Z}_t = \text{GNN}(f_{\text{temp}}(\mathbf{X}_t, \mathbf{H}_{t-1}), \mathcal{E}_t) \quad (1)$$

where f_{temp} is a recurrent or attention-based temporal encoder.

Definition 3.3 (Spatial-first paradigm). *The spatial-first paradigm computes*

$$\mathbf{Z}_t = f_{\text{temp}}(\text{GNN}(\mathbf{X}_t, \mathcal{E}_t), \mathbf{H}_{t-1}) \quad (2)$$

4 The SiST-GNN Architecture

We now formalize our SiST-GNN layer, instantiate its temporal encoder, and analyze complexity.

4.1 Temporal Encoder

Each node v keeps hidden and cell states $(\mathbf{h}_v^{(t)}, \mathbf{c}_v^{(t)}) \in \mathbb{R}^{d_h} \times \mathbb{R}^{d_h}$ that summarise its trajectory up to snapshot $t - 1$. At snapshot t the LSTM cell Hochreiter & Schmidhuber (1997) consumes the current feature vector and updates the states,

$$(\mathbf{h}_v^{(t)}, \mathbf{c}_v^{(t)}) = \text{LSTMCell}(\mathbf{x}_v^{(t)}, (\mathbf{h}_v^{(t-1)}, \mathbf{c}_v^{(t-1)})) \quad (3)$$

and we set the temporal summary to the current hidden state, $\tilde{\mathbf{x}}_v^{(t)} \equiv \mathbf{h}_v^{(t)}$. The LSTM cell is shared across all N nodes (its parameters do not scale with $|\mathcal{V}|$) and is applied row-wise, which preserves the permutation equivariance of the layer (Lemma 4.3). We follow standard truncated BPTT Williams & Peng (1990): hidden and cell states are detached after every backward pass to bound the temporal credit-assignment window and to keep per-snapshot memory constant in T .

4.2 Temporally Augmented Graph

Definition 4.1 (Augmented graph). *Given $\mathcal{G}_t = (\mathcal{V}_t, \mathcal{E}_t)$ with $|\mathcal{V}_t| = N$, the temporally augmented graph is $\hat{\mathcal{G}}_t = (\hat{\mathcal{V}}_t, \hat{\mathcal{E}}_t)$ with*

$$\hat{\mathcal{V}}_t = \{1, \dots, N\} \cup \{N+1, \dots, 2N\} \quad (4)$$

$$\hat{\mathcal{E}}_t = \mathcal{E}_t \cup \{(u + N, v) \mid (u, v) \in \mathcal{E}_t\} \cup \{(u + N, u) \mid u \in \mathcal{V}_t\} \quad (5)$$

$$\mathbf{X}_{\text{aug}} = [\text{proj}(\mathbf{X}_t); \tilde{\mathbf{X}}_t] \quad (6)$$

where $\text{proj}(\mathbf{X}_t)$ is the projected node features in d_h dimension and $\tilde{\mathbf{X}}_t$ is the temporal encoded features.

The cross-time edges $(u + N, v)$ and $(u + N, u)$ allow node u to receive directly, via one round of standard message passing, the temporal summary of its neighbor v and itself. Only original edges (intra-time edges) induce cross-time edges, so the augmented graph is always a sparse perturbation of the input ($|\hat{\mathcal{E}}_t| = 2|\mathcal{E}_t| + N$).

4.3 Forward Pass

One SiST-GNN layer computes

$$\mathbf{Z}_t = \sigma \left(\text{GNN}(\mathbf{X}_{\text{aug}}, \hat{\mathcal{E}}_t)_{[1:N]} \right) \quad (7)$$

where the σ operator is element-wise nonlinearity. The first N rows of the GNN output are the next-layer input; the lower N rows are discarded. Algorithm 1 gives the full single-snapshot procedure. When L layers are stacked, each layer keeps its own recurrent state, and the cross-time edges are re-instantiated at every depth.

4.4 From Layers to Link Prediction

SiST-GNN layer outputs node representation \mathbf{Z}_t at every snapshot. To turn the layer into a full link-prediction model, we (i) give every node an identity-aware feature vector, (ii) stack L SiST-GNN layers to form an encoder, and (iii) score candidate edges with a parameter-free inner-product decoder.

Input features. Following the ROLAND convention, the raw per-snapshot input is a constant feature $(\mathbf{1} \in \mathbb{R}^{N \times 1})$ plus per-node *learnable* embeddings $\mathbf{P} \in \mathbb{R}^{N \times d_h}$ that are trained jointly with the model. At every snapshot t , we feed $\mathbf{X}_t = \mathbf{P}$ as the input to the first SiST-GNN layer.

Encoder. The encoder is an L -layer stack of SiST-GNN layers. Each layer maintains its own $(\mathbf{H}_t^{(\ell)}, \mathbf{C}_t^{(\ell)})$, and the output of layer ℓ feeds the input of layer $\ell+1$. A ReLU nonlinearity and dropout are applied between consecutive layers. The final layer’s output for the first N nodes, $\mathbf{Z}_t = \text{SiST}^{(L)}(\mathbf{X}_t, \mathcal{E}_t)$, is the node embedding used for downstream prediction.

Algorithm 1 SiST-GNN layer, single snapshot.

Require: Features $\mathbf{X}_t \in \mathbb{R}^{N \times d}$; the COO encoding $\mathbf{E}_t \in \mathbb{Z}^{2 \times |\mathcal{E}_t|}$ of the edge set \mathcal{E}_t (column k holds the endpoints of the k -th edge); prior states $\mathbf{H}_{t-1}, \mathbf{C}_{t-1} \in \mathbb{R}^{N \times d_h}$.

Ensure: Output $\mathbf{Z}_t \in \mathbb{R}^{N \times d_h}$, updated states $\mathbf{H}_t, \mathbf{C}_t$.

- 1: $\mathbf{H}_t, \mathbf{C}_t \leftarrow \text{LSTMCell}(\mathbf{X}_t, (\mathbf{H}_{t-1}, \mathbf{C}_{t-1}))$ ▷ Temporal update
 - 2: $\mathbf{X}_{\text{proj}} \leftarrow W_p \mathbf{X}_t$ ▷ Project to d_h
 - 3: $\mathbf{X}_{\text{aug}} \leftarrow [\mathbf{X}_{\text{proj}}; \mathbf{H}_t]$ ▷ $2N \times d_h$
 - 4: $\hat{\mathbf{E}}_t \leftarrow [\mathbf{E}_t \| (\mathbf{E}_t^{[0,:]} + N, \mathbf{E}_t^{[1,:]}) \| \{(N+i, i)\}_{i=1}^N]$ ▷ Append cross-time columns (N -shifted source)
 - 5: $\mathbf{X}' \leftarrow \text{GNN}(\mathbf{X}_{\text{aug}}, \hat{\mathbf{E}}_t)$ ▷ Joint message passing
 - 6: $\mathbf{Z}_t \leftarrow \sigma(\mathbf{X}'_{[1:N]})$ ▷ Slice original nodes
 - 7: **return** $\mathbf{Z}_t, \mathbf{H}_t, \mathbf{C}_t$
-

Inner-product decoder. For any candidate edge $(u, v) \in \mathcal{V} \times \mathcal{V}$ the score is

$$s_t(u, v) = \langle \mathbf{z}_u^{(t)}, \mathbf{z}_v^{(t)} \rangle \quad (8)$$

For each positive edge $(u, v) \in \mathcal{E}_t$ we sample one negative tail $v^- \sim \text{Uniform}(\mathcal{V}_t)$ during training and 1000 negative tails during evaluation, computing the mean reciprocal rank (MRR) of the positive against the negatives.

Loss. We optimize the margin-ranking loss with unit margin, summed over the positive edges of the current snapshot:

$$\mathcal{L}_t = \frac{1}{|\mathcal{E}_t|} \sum_{(u,v) \in \mathcal{E}_t} \max\left(0, 1 - s_t(u, v) + s_t(u, v^-)\right). \quad (9)$$

Truncated BPTT over snapshots. At every snapshot we (a) run the encoder forward, (b) back-propagate over \mathcal{L}_t , (c) detach every per-layer $(\mathbf{H}_t^{(\ell)}, \mathbf{C}_t^{(\ell)})$ from the computation graph before moving to snapshot $t+1$. This bounds the credit-assignment horizon to a single snapshot and makes the per-snapshot memory cost constant in T . It is the same truncation used by ROLAND’s incremental scheme.

4.5 From Layers to Dynamic Node Classification

The same SiST-GNN encoder is used for a node-classification model with only the readout, loss, and input-feature pipeline changing.

Discretizing continuous-time interactions. The JODIE-style benchmarks (Wikipedia, Reddit, MOOC) are released as continuous-time bipartite interaction streams $\{(u_k, v_k, t_k, \mathbf{e}_k, y_k)\}_{k=1}^{|\mathcal{E}|}$, where $\mathbf{e}_k \in \mathbb{R}^{d_e}$ is the edge feature and $y_k \in \{0, 1\}$ is the state-change label of the source node u_k at time t_k . To bring the data into the snapshot setting required by our encoder we bin all interactions into fixed-width windows of Δ hours, indexed $t = 1, \dots, T$; the snapshot graph \mathcal{G}_t is the multigraph of interactions whose timestamps fall in $[(t-1)\Delta, t\Delta)$, and a node carries its (constant) raw feature in every snapshot. We sweep $\Delta \in \{1, 3, 6, 12, 24\}$ h (Figure 3a) and default to $\Delta = 6$ h. Discretization is a clear modeling choice, not a free lunch: it trades the fine-grained event ordering used by continuous-time models Rossi et al. (2020); da Xu et al. (2020) for a uniform snapshot interface that fits our augmented-graph construction without modification. We discuss the implications in Section 6.

Input features. Each node receives its dataset-provided static feature $\mathbf{f}_v \in \mathbb{R}^{d_f}$ plus a learnable per-node embedding $\mathbf{p}_v \in \mathbb{R}^{d_h}$, projected and summed into a single \mathbb{R}^{d_h} vector that is fed to the first SiST-GNN layer. Edge features \mathbf{e}_k are encoded by a two-layer MLP whose output is fused into the source representation through a residual connection before the readout; this lets the head condition on the most recent interaction context within the current snapshot.

Readout and loss. The encoder produces \mathbf{Z}_t which then used as input for a two-layer MLP $\phi : \mathbb{R}^{d_h} \rightarrow \mathbb{R}$ scores each source node, $\hat{y}_v^{(t)} = \sigma(\phi(\mathbf{z}_v^{(t)}))$, and we optimise the (weighted) binary cross-entropy

$$\mathcal{L}_t^{\text{NC}} = -\frac{1}{|\mathcal{S}_t|} \sum_{v \in \mathcal{S}_t} \left(w^+ y_v^{(t)} \log \hat{y}_v^{(t)} + (1 - y_v^{(t)}) \log(1 - \hat{y}_v^{(t)}) \right) \quad (10)$$

where \mathcal{S}_t is the set of source nodes that emit at least one interaction in snapshot t . Following standard practice on these benchmarks we set $w^+ = |\mathcal{S}_t^-|/|\mathcal{S}_t^+|$ (*balanced* BCE) to compensate for the extreme positive-class imbalance. The same truncated-BPTT schedule of Section 4.4 is used: hidden and cell states are detached between snapshots.

4.6 Theoretical Properties

We prove four properties of the SiST-GNN layer: a counting argument that quantifies the additional messages it propagates per layer (Proposition 4.1); two reduction lemmas that show two stacked SiST-GNN layers can simulate either of the sequential paradigms of Section 3 (Lemmas 4.1 and 4.2); a strict-generalization theorem that follows from the lemmas together with an explicit witness (Theorem 4.1); and permutation equivariance (Lemma 4.3).

Architectural enabler. The reduction lemmas rest on a standard assumption from heterogeneous-edge GNNs: the spatial backbone treats the three edge types of $\hat{\mathcal{E}}_t$ as separately weighted. We model this by three scalar gates $\alpha_{\text{intra}}, \alpha_{\text{cross}}, \alpha_{\text{self}} \in \mathbb{R}$, each multiplying the contribution of one edge type to the aggregation sum, with all three equal to 1 as the default; setting a gate to 0 drops the corresponding messages. The three scalars add no asymptotic complexity and are subsumed by per-edge-type weight matrices in any standard message-passing backbone (GCN, GraphSAGE, GAT, GIN).

Recurrence assumption. We further assume the temporal cell f_{temp} admits an *identity parameterization*: a setting of its parameters under which $f_{\text{temp}}(\mathbf{x}, \mathbf{h}) = \mathbf{h}$ for every (\mathbf{x}, \mathbf{h}) . This is satisfied by every gated recurrent variant used in the DGNN literature; for the LSTM, the forget gate is driven to 1, the input gate to 0, and the output gate aligned with the cell-state activation.

Proposition 4.1 (Message diversity). *Fix snapshot t and node $u \in \{1, \dots, N\}$. In a SiST-GNN layer, node u receives exactly*

$$2|\mathcal{N}(u)| + 1$$

incoming messages in $\hat{\mathcal{G}}_t$: one per spatial neighbor (intra-time), one per cross-time copy of a spatial neighbor, and one cross-time self message. For every neighbor $v \in \mathcal{N}(u)$, the two messages originating from v carry feature vectors $(\mathbf{X}_t \mathbf{W}_p)[v, :]$ and $\tilde{\mathbf{x}}_v^{(t)}$, which are not expressible as a common function of $\mathbf{x}_v^{(t)}$ alone, so the layer can assign them independent aggregation weights. A spatial-first or temporal-first DGNN with the same backbone produces at most $|\mathcal{N}(u)| + 1$ messages per layer, each carrying a single composite feature.

Proof. The count is direct from Definition 4.1: $\hat{\mathcal{E}}_t$ contains $|\mathcal{E}_t|$ intra-time edges, $|\mathcal{E}_t|$ cross-time neighbor edges, and N cross-time self edges, of which $|\mathcal{N}(u)|$, $|\mathcal{N}(u)|$, and 1, respectively, are incident to u .

For distinguishability, note that $(\mathbf{X}_t \mathbf{W}_p)[v, :]$ is a linear function of $\mathbf{x}_v^{(t)}$ alone, while $\tilde{\mathbf{x}}_v^{(t)} = \mathbf{h}_v^{(t)}$ depends on the full history $\mathbf{x}_v^{(1)}, \dots, \mathbf{x}_v^{(t)}$ through the recurrence. Pick any $t \geq 2$ and any two histories that agree at t but differ at $t-1$; the projected feature coincides on the two histories while $\mathbf{h}_v^{(t)}$ does not (for any non-degenerate f_{temp}). Hence, no function of $\mathbf{x}_v^{(t)}$ alone can equal both messages, so the aggregator is free to weight them independently.

In a sequential DGNN with the same backbone, each per-layer message-passing step produces one message per spatial neighbor plus a recurrent self-update, totaling $|\mathcal{N}(u)| + 1$ messages, and each message already collapses the spatial and temporal views into a single feature. \square

The doubled message pool is the mechanism by which the message-passing operator can, at inference time, weight a neighbor’s present features and its historical trajectory differently for the prediction of an edge or a node, without any architectural change.

Lemma 4.1 (Spatial-first recovery). *There exist parameter settings of two stacked SiST-GNN layers under which, for every $t \geq 1$ and every initial state \mathbf{H}_0 , the layer-2 output equals the spatial-first function $\mathbf{Z}_t = f_{\text{temp}}(\text{GNN}(\mathbf{X}_t, \mathcal{E}_t), \mathbf{H}_{t-1})$ of Definition 3.3.*

Proof. Let $(\mathbf{H}_t^{(\ell)}, \mathbf{C}_t^{(\ell)})$ denote the LSTM state of layer $\ell \in \{1, 2\}$ at snapshot t . We construct parameters such that

$$\mathbf{Z}_t^{(1)} = \text{GNN}(\mathbf{X}_t, \mathcal{E}_t), \quad \mathbf{Z}_t^{(2)} = f_{\text{temp}}(\mathbf{Z}_t^{(1)}, \mathbf{H}_{t-1}^{(2)}),$$

and verify that $\mathbf{H}_{t-1}^{(2)}$ tracks the spatial-first reference state at every t .

Layer 1. Set $\alpha_{\text{intra}}^{(1)} = 1$ and $\alpha_{\text{cross}}^{(1)} = \alpha_{\text{self}}^{(1)} = 0$, so the GNN ignores all cross-time edges and operates on the upper half of \mathbf{X}_{aug} , i.e. on $\mathbf{X}_t \mathbf{W}_p^{(1)}$ over \mathcal{E}_t . Choose $\mathbf{W}_p^{(1)}$ together with the GNN’s own input map to realize the spatial-first reference GNN: every standard message-passing backbone has a learnable input linear map, so the composition $(\mathbf{X}_t \mathbf{W}_p^{(1)}) \mapsto \text{GNN}(\cdot)$ expresses the same function class as the reference $\text{GNN}(\mathbf{X}_t, \cdot)$. Set the post-aggregation nonlinearity $\sigma^{(1)}$ to the identity (or fold it into the backbone, which is standard). The state $(\mathbf{H}_t^{(1)}, \mathbf{C}_t^{(1)})$ is updated by the layer-1 LSTM but is read by no downstream computation, so its parameters are free; the layer-1 output is $\mathbf{Z}_t^{(1)} = \text{GNN}(\mathbf{X}_t, \mathcal{E}_t)$.

Layer 2. Set $\alpha_{\text{intra}}^{(2)} = \alpha_{\text{cross}}^{(2)} = \alpha_{\text{self}}^{(2)} = 0$ and the layer-2 GNN’s self-loop weight matrix to \mathbf{I} , with all neighbor weights zero. Every standard backbone (GCN, GraphSAGE, GAT) realizes the identity under this parameterization; the upper half of \mathbf{X}_{aug} then passes through unchanged. With $\mathbf{W}_p^{(2)} = \mathbf{I}$ and $\sigma^{(2)} = \text{id}$, the layer-2 output is $\mathbf{Z}_t^{(2)} = f_{\text{temp}}(\mathbf{Z}_t^{(1)}, \mathbf{H}_{t-1}^{(2)})$.

State alignment, by induction on t . Initialize $\mathbf{H}_0^{(2)} = \mathbf{H}_0$. At $t = 1$, $\mathbf{Z}_1^{(2)} = f_{\text{temp}}(\text{GNN}(\mathbf{X}_1, \mathcal{E}_1), \mathbf{H}_0)$, which matches the spatial-first output at $t = 1$ exactly. The layer-2 LSTM then produces $\mathbf{H}_1^{(2)}$ by applying f_{temp} to the same arguments, which by definition coincides with the spatial-first reference state \mathbf{H}_1 . The induction step from t to $t + 1$ is identical. \square

Lemma 4.2 (Temporal-first recovery). *There exist parameter settings of two stacked SiST-GNN layers under which, for every $t \geq 1$ and every initial state \mathbf{H}_0 , the layer-2 output equals the temporal-first function $\mathbf{Z}_t = \text{GNN}(f_{\text{temp}}(\mathbf{X}_t, \mathbf{H}_{t-1}), \mathcal{E}_t)$ of Definition 3.2.*

Proof. Set $\alpha_{\text{cross}}^{(1)} = \alpha_{\text{self}}^{(1)} = 1$ and $\alpha_{\text{intra}}^{(1)} = 0$. This essentially results in GNN ignoring all intra-time edges and operating on the lower half of \mathbf{X}_{aug} , i.e., on $\tilde{\mathbf{X}}_t = f_{\text{temp}}(\mathbf{X}_t^{(1)}, \mathbf{H}_{t-1}^{(1)})$. Hence, the final output of this modified SiST-GNN Layer becomes $\mathbf{Z}_t = \text{GNN}(f_{\text{temp}}(\mathbf{X}_t^{(1)}, \mathbf{H}_{t-1}^{(1)}))$ which matches the Definition 3.2 \square

Theorem 4.1 (Strict generalization). *Let $\mathcal{F}_{\text{SiST}}$, $\mathcal{F}_{\text{S} \rightarrow \text{T}}$, and $\mathcal{F}_{\text{T} \rightarrow \text{S}}$ denote the function classes computed, respectively, by SiST-GNN stack, by a spatial-first DGNN, and by a temporal-first DGNN, all sharing a fixed backbone GNN and a fixed recurrence f_{temp} . Then*

$$\mathcal{F}_{\text{S} \rightarrow \text{T}} \cup \mathcal{F}_{\text{T} \rightarrow \text{S}} \subsetneq \mathcal{F}_{\text{SiST}}.$$

Proof. Inclusion. Lemmas 4.1 and 4.2 give, for every $g \in \mathcal{F}_{\text{S} \rightarrow \text{T}} \cup \mathcal{F}_{\text{T} \rightarrow \text{S}}$, an explicit parameter setting of a two-layer SiST-GNN stack that computes g .

Strictness, by example. To show that there are functions in $\mathcal{F}_{\text{SiST}}$ that cannot be represented by functions in $\mathcal{F}_{\text{S} \rightarrow \text{T}}$, or $\mathcal{F}_{\text{T} \rightarrow \text{S}}$, we will construct a counterexample.

Let us assume the GNN operator as a function f defined as $f(X) = AXW$, where A is an adjacency matrix of dimension $N \times N$, X and W are the feature and weight matrix. Let us also assume g as the temporal operator. The GNN module of $\mathcal{F}_{\text{SiST}}$ require an adjacency matrix A' of dimension $2N \times 2N$, which can be broken down into 4 blocks as $A' = \begin{pmatrix} A_{11} & A_{12} \\ A_{21} & A_{22} \end{pmatrix}$, similarly, $\mathbf{X}_{\text{aug}} = \begin{pmatrix} X \\ g(X, H) \end{pmatrix}$. The top $N \times d_h$ block of SiST-GNN would be like:

$$\text{SiST-GNN}(X) = Y(X) = A_{11}XW + A_{12}g(X)W \tag{11}$$

Let $N = 2$, $d_h = 1$ and $W = [1]$. The input matrix will be a column matrix $X = \begin{pmatrix} x_1 \\ x_2 \end{pmatrix}$. For simplicity, let's assume the temporal operator requires no hidden state. Let us assume the row-wise temporal operator be as a square operation $g(X) = \begin{pmatrix} x_1^2 \\ x_2^2 \end{pmatrix}$. Consider $A_{11} = \begin{pmatrix} 0 & 1 \\ 1 & 0 \end{pmatrix}$ and $A_{12} = \begin{pmatrix} 1 & 0 \\ 0 & 1 \end{pmatrix}$. Substituting these in Equation 11, we get the following:

$$Y(X) = \begin{pmatrix} 0 & 1 \\ 1 & 0 \end{pmatrix} \begin{pmatrix} x_1 \\ x_2 \end{pmatrix} + \begin{pmatrix} 1 & 0 \\ 0 & 1 \end{pmatrix} \begin{pmatrix} x_1^2 \\ x_2^2 \end{pmatrix} = \begin{pmatrix} x_2 + x_1^2 \\ x_1 + x_2^2 \end{pmatrix}$$

Case T \rightarrow S. Any function in $\mathcal{F}_{T \rightarrow S}$ has the form $f(g(X)) = A_{TS} \cdot g_{TS}(X) W_{TS}$. Because $d_h = 1$, W_{TS} can be absorbed into g_{TS} . Since g_{TS} is a row wise operation, X can be mapped to $\begin{pmatrix} \phi_1(x_1) \\ \phi_2(x_2) \end{pmatrix}$. Let $A_{TS} = \begin{pmatrix} a & b \\ c & d \end{pmatrix}$. The general form of a $\mathcal{F}_{T \rightarrow S}$ function can be written as:

$$Y_{TS}(X) = \begin{pmatrix} a & b \\ c & d \end{pmatrix} \begin{pmatrix} \phi_1(x_1) \\ \phi_2(x_2) \end{pmatrix} = \begin{pmatrix} a\phi_1(x_1) + b\phi_2(x_2) \\ c\phi_1(x_1) + d\phi_2(x_2) \end{pmatrix}$$

For this to match our target function $Y(X)$, we set up the following equation:

$$a\phi_1(x_1) + b\phi_2(x_2) = x_1^2 + x_2, \quad c\phi_1(x_1) + d\phi_2(x_2) = x_1 + x_2^2$$

There cannot exist any ϕ_1 and ϕ_2 satisfying the above equation for constant a, b, c, d . There a function in $\mathcal{F}_{\text{SiST}}$ that does not exist in $\mathcal{F}_{T \rightarrow S}$.

Case S \rightarrow T. Any function in $\mathcal{F}_{S \rightarrow T}$ has the form $g_{ST}(f(X)) = g_{TS}(A_{ST} X W_{ST})$. Using $A_{ST} = A_{TS}$, we can write the following:

$$Y_{ST}(X) = \begin{pmatrix} \psi_1(ax_1 + bx_2) \\ \psi_2(cx_1 + dx_2) \end{pmatrix}$$

Similarly, to match our target equation, we get the following equation:

$$\psi_1(ax_1 + bx_2) = x_1^2 + x_2, \quad \psi_2(cx_1 + dx_2) = x_1 + x_2^2$$

The gradient component for the left side of both equations is either constant or undefined; however, for the right side of the equation, the gradient component varies with either x_1 or x_2 . Thus, our target function cannot be represented using a function from $\mathcal{F}_{T \rightarrow S}$.

Combining the two cases completes the strict inclusion. \square

Lemma 4.3 (Permutation equivariance). *For every permutation π of $\{1, \dots, N\}$ with matrix \mathbf{P}_π , the SiST-GNN layer satisfies*

$$\begin{aligned} & \text{SiST-GNN}(\mathbf{P}_\pi \mathbf{X}_t, \pi(\mathcal{E}_t), \mathbf{P}_\pi \mathbf{H}_{t-1}, \mathbf{P}_\pi \mathbf{C}_{t-1}) \\ &= \mathbf{P}_\pi \cdot \text{SiST-GNN}(\mathbf{X}_t, \mathcal{E}_t, \mathbf{H}_{t-1}, \mathbf{C}_{t-1}) \end{aligned}$$

and the same identity holds simultaneously for the updated states \mathbf{H}_t and \mathbf{C}_t .

Proof. Define $\hat{\pi} : \{1, \dots, 2N\} \rightarrow \{1, \dots, 2N\}$ by $\hat{\pi}(u) = \pi(u)$ for $u \leq N$ and $\hat{\pi}(u + N) = \pi(u) + N$. Then $\hat{\pi}$ is a permutation of the augmented node set with matrix $\mathbf{P}_{\hat{\pi}} = \text{diag}(\mathbf{P}_\pi, \mathbf{P}_\pi)$.

(i) *Temporal update.* The LSTM cell is applied row-wise to \mathbf{X}_t ; any row-wise map commutes with any row permutation, so the layer-1 LSTM state becomes $(\mathbf{P}_\pi \mathbf{H}_t, \mathbf{P}_\pi \mathbf{C}_t)$ under permuted input.

(ii) *Stacking.* $\mathbf{X}_{\text{aug}} = [\mathbf{X}_t \mathbf{W}_p; \mathbf{H}_t] \in \mathbb{R}^{2N \times d_h}$. Under permuted input the upper block becomes $\mathbf{P}_\pi \mathbf{X}_t \mathbf{W}_p$ and the lower block $\mathbf{P}_\pi \mathbf{H}_t$, which is exactly $\mathbf{P}_{\hat{\pi}} \mathbf{X}_{\text{aug}}$.

(iii) *Edge augmentation.* The augmentation map of Definition 4.1 depends only on the unordered edge set:

$$\widehat{\pi(\mathcal{E}_t)} = \pi(\mathcal{E}_t) \cup \{(\pi(u) + N, \pi(v)) : (u, v) \in \mathcal{E}_t\} \cup \{(\pi(u) + N, \pi(u)) : u \in \mathcal{V}_t\} = \hat{\pi}(\hat{\mathcal{E}}_t),$$

Table 1: Per-snapshot, per-layer complexity. SiST-GNN’s overhead over comparable spatial-first models is a fixed $2\times$ factor on the message-passing term, plus an LSTMCell, which any temporally-aware baseline already pays for. Below, “DZP” denotes the cost of computing Dowker-Zigzag persistence diagrams in TMetaNet.

Model	Compute	Act. mem.	Rec. state
GCN Kipf & Welling (2017)	$Ed_h + Nd_h^2$	Nd_h	—
EvolveGCN Pareja et al. (2020)	$Ed_h + Nd_h^2$	Nd_h	d_h^2
GCRN Seo et al. (2018)	$Ed_h + Nd_h^2$	Nd_h	Nd_h
T-GCN Zhao et al. (2020)	$Ed_h + Nd_h^2$	Nd_h	Nd_h
ROLAND-GRU You et al. (2022)	$Ed_h + Nd_h^2$	Nd_h	Nd_h
TMetaNet Li et al. (2025)	$Ed_h + Nd_h^2 + \text{DZP}$	Nd_h	Nd_h
SiST-GNN (ours)	$Ed_h + Nd_h^2$	$2Nd_h$	Nd_h

so re-running the augmentation on $\pi(\mathcal{E}_t)$ produces exactly the $\hat{\pi}$ -image of $\hat{\mathcal{E}}_t$.

(iv) *Message passing.* Every standard message-passing GNN is permutation-equivariant on its node set Kipf & Welling (2017); Veličković et al. (2018); Hamilton et al. (2017); Xu et al. (2019); applying this with the permutation $\hat{\pi}$ on the augmented domain,

$$\text{GNN}(\mathbf{P}_{\hat{\pi}}\mathbf{X}_{\text{aug}}, \hat{\pi}(\hat{\mathcal{E}}_t)) = \mathbf{P}_{\hat{\pi}} \text{GNN}(\mathbf{X}_{\text{aug}}, \hat{\mathcal{E}}_t).$$

(v) *Slicing.* Because $\hat{\pi}$ maps $\{1, \dots, N\}$ to itself and restricts there to π , the row-permutation $\mathbf{P}_{\hat{\pi}}$ acts as \mathbf{P}_{π} on the first N rows. The element-wise σ commutes with any row permutation. Hence $\mathbf{Z}_t = \sigma(\mathbf{X}'_{1:N, :})$ transforms as $\mathbf{P}_{\pi}\mathbf{Z}_t$.

Combining (i)–(v) gives the stated equivariance for \mathbf{Z}_t , and (i) gives it simultaneously for $\mathbf{H}_t, \mathbf{C}_t$. \square

4.7 Complexity

Let a spatial-first baseline with the same backbone process N nodes and E edges per snapshot in $O(Nd_h^2 + Ed_h)$ time. One SiST-GNN layer requires: (i) one LSTMCell pass at $O(Nd_h^2)$, identical to the baseline’s temporal module; (ii) one graph convolution over $2N$ nodes and $2E + N$ edges at $O(Nd_h^2 + Ed_h)$, asymptotically equal to the baseline; and (iii) $O(Nd_h)$ additional activation memory for the stacked features. The per-snapshot time and memory cost is therefore within a constant factor of any spatial-first baseline with the same hidden dimension.

In practice, the constant factor is amortized by using fewer stacked layers (our 2-layer SiST-GNN outperforms deeper baselines), and the LSTMCell overhead is dominated by the GNN.

4.8 Evaluation Protocols

We adopt the two evaluation protocols introduced by ROLAND You et al. (2022) for the link prediction task, and another evaluation protocol Kumar et al. (2019); da Xu et al. (2020) for the node classification task.

Fixed-split. The first 90% of snapshots are used to train the model; the remaining 10% are held out for evaluation. The model processes the training sequence in temporal order, carrying recurrent states across snapshots and detaching them after every backward step.

Live-update. At each snapshot t , the model *first* predicts links on \mathcal{G}_t using states from $t-1$, *then* trains on \mathcal{G}_t for a fixed budget of K inner epochs. This mirrors the online-deployment regime in which a model must commit to predictions before observing the new ground truth, and it isolates the *adaptation* component of the model from its long-horizon training behavior.

In both protocols, the loss is equation 9 and the metric is MRR computed snapshot-by-snapshot.

Table 2: Dataset statistics. $|\mathcal{V}|$ and $|\mathcal{E}|$ are total unique nodes and edges across all snapshots; T is the number of snapshots.

Dataset	$ \mathcal{V} $	$ \mathcal{E} $	T	Domain
Bitcoin-OTC Kumar et al. (2016)	5,881	35,592	279	Trust network
Bitcoin-Alpha Kumar et al. (2016)	3,783	24,186	274	Trust network
UCI-Message Panzarasa et al. (2009)	1,899	59,835	29	Communication
Reddit-Title Kumar et al. (2018)	35,776	286,561	178	Hyperlink graph
Reddit-Body Kumar et al. (2018)	35,776	286,561	178	Hyperlink graph
AS-733 Leskovec et al. (2005)	7,716	26,467	733	Internet AS

Table 3: Dynamic node-classification dataset statistics. The JODIE benchmarks are released as continuous-time bipartite event streams. T_Δ is the number of snapshots after discretizing at the default bucket width $\Delta = 6$ h; positive-rate is the fraction of source nodes whose state-change label is 1.

Dataset	$ \mathcal{V} $	$ \mathcal{E} $	T_Δ	pos. rate	Domain
Wikipedia	8,227	157,474	124	0.14%	Edit logs
Reddit	10,000	672,447	124	0.05%	Posts
MOOC	7,047	411,749	120	0.99%	E-learning

Node classification split. We use a chronological train/validation /test split of 70/15/15% of snapshots and report test AUC.

5 Experiments

5.1 Datasets

We evaluate on *two* task families. For dynamic **link prediction** we use the six public datasets for snapshot DGNNs You et al. (2022); Zhu et al. (2023); Li et al. (2025) (Table 2). **Bitcoin-OTC** and **Bitcoin-Alpha** are who-trusts-whom signed networks from two Bitcoin trading platforms. **UCI-Message** records private messages between students at UC Irvine. **Reddit-Title** and **Reddit-Body** capture hyperlink interactions between subreddit communities. **AS-733** consists of daily snapshots of the Internet autonomous-system topology. Following ROLAND You et al. (2022), we discretize Bitcoin, UCI, and Reddit into weekly snapshots, and AS-733 into daily snapshots; the same snapshot frequencies are used by all methods.

For dynamic **node classification** we use the three continuous-time JODIE benchmark Kumar et al. (2019) datasets – Wikipedia, Reddit, and MOOC – discretized into fixed-width snapshots (Table 3). **Wikipedia** records edits by users on Wikipedia pages over a one-month window; the binary label is whether the editing user is subsequently banned. **Reddit** records users’ posts to subreddits over the same window; the label indicates whether the user is later banned from posting. **MOOC** records student interactions with online-course units; the label is whether the student subsequently drops the course. All three are released as continuous-time streams Kumar et al. (2019); we discretize them into $\Delta = 6$ h snapshots.

5.2 Baselines

5.2.1 Link Prediction

We compare against fourteen methods spanning every major DGNN family:

- **Static.** GCN Kipf & Welling (2017) trained on the final snapshot.
- **Dynamic embeddings.** DynGEM Goyal et al. (2018), dyngraph2vecAE and dyn-graph2vecAERNN Goyal et al. (2020).
- **Temporal-first.** EvolveGCN-H, EvolveGCN-O Pareja et al. (2020).

- **Spatial-first.** GCRN-GRU, GCRN-LSTM and GCRN - Baseline Seo et al. (2018); T-GCN Zhao et al. (2020); the three ROLAND variants Moving-Average, MLP-Update and GRU-Update You et al. (2022).
- **Meta-learning.** TMetaNet Li et al. (2025)

Every experiment is repeated with five random seeds, and we report the mean MRR and standard deviation of MRR.

5.2.2 Node Classification

We compare SiST-GNN against two families of dynamic-GNN methods.

- **CTDG based models.** They consume the native continuous-time event stream and are therefore the harder comparison for any snapshot-based approach: JODIE Kumar et al. (2019), TGN Rossi et al. (2020), DyREP Trivedi et al. (2019), TGAT da Xu et al. (2020), and APAN Wang et al. (2021b).
- **DTDG based models.** They operate on the same discretized snapshot sequence as SiST-GNN: EvolveGCN-H and EvolveGCN-O Pareja et al. (2020), ROLAND You et al. (2022), a DTDG-adapted TGN Rossi et al. (2020), the Hawkes-process-based TREND Wen & Fang (2022), and the MLP-mixer GraphMixer Cong et al. (2023).

CTDG baseline numbers and the two EvolveGCN entries are reproduced from the survey Feng et al. (2026); the remaining DTDG baselines follow their original AUC protocol. We do *not* compare against pre-training or prompt-based methods Yu et al. (2025), as they rely on a different upstream pre-training phase that is incompatible with our supervised pipeline; we revisit this gap in Section 6.

5.3 Implementation

SiST-GNN is implemented in PyTorch Paszke et al. (2019) and PyTorch Geometric Fey & Lenssen (2019). For the link prediction task, our default configuration is a 2-layer SiST-GNN with GCNConv as the spatial backbone, hidden dimension $d_h = 128$, learnable node embeddings of dimension 128, dropout 0.1, and the Adam optimiser Kingma & Ba (2015) with learning rate 10^{-3} and weight decay 10^{-5} . We train for 100 epochs.

For node classification task, our configuration is $\Delta = 6$ h, $L = 2$ layers, $d_h = 256$, GCNConv backbone, *balanced* BCE loss, 100 epochs and early stopping with patience 5, Adam at 10^{-3} . The link-prediction head, loss, and negative-sampling protocol are described in Section 4.4; we use them unchanged.

The device configurations are Intel(R) Xeon(R) Gold 5120 CPU @ 2.20 GHz, 256 GB RAM, NVIDIA A100 40GB GPU. The source code is available at this  Github Repository

5.4 Link Prediction Results

5.4.1 Fixed-Split Results

Table 5 reports MRR on the three datasets used in ROLAND’s fixed-split evaluation. SiST-GNN attains 0.830 on Bitcoin-OTC, 0.773 on Bitcoin-Alpha, and 0.480 on UCI-Message, dominating the previous best (ROLAND GRU) by +277.2%, +167.4%, and +109.6%, respectively. The relative gain is largest on the denser, more strongly recurrent Bitcoin trust networks, where each edge carries a strong signal about future ratings; on UCI-Message, where interactions are sparser and less repetitive, the gain is more modest but still significant.

5.4.2 Live-Update Results

Table 4 reports the live-update results across all six benchmarks. SiST-GNN achieves a state-of-the-art result across all datasets. Three observations stand out. Relative gains over the baseline range from +68.6% on Reddit-Title to

Table 4: Live-update MRR (mean \pm std. over 5 seeds). Top: baselines with standard BPTT training. Middle: baselines with ROLAND incremental training. Bottom: ROLAND variants, TMetaNet, and SiST-GNN. OOM = out-of-memory after five retries; Best per column in **bold**.

	AS-733	Reddit-Title	Reddit-Body	UCI-Message	Bitcoin-OTC	Bitcoin-Alpha
<i>Baselines with standard training (BPTT)</i>						
EvolveGCN-H Pareja et al. (2020)	OOM	OOM	0.148 \pm 0.013	0.061 \pm 0.040	0.067 \pm 0.035	0.079 \pm 0.032
EvolveGCN-O Pareja et al. (2020)	OOM	OOM	OOM	0.071 \pm 0.009	0.085 \pm 0.022	0.071 \pm 0.025
GCRN-GRU Seo et al. (2018)	OOM	OOM	OOM	0.080 \pm 0.012	OOM	OOM
GCRN-LSTM Seo et al. (2018)	OOM	OOM	OOM	0.083 \pm 0.001	OOM	OOM
GCRN-Baseline Seo et al. (2018)	OOM	OOM	OOM	0.069 \pm 0.004	0.152 \pm 0.011	0.141 \pm 0.005
T-GCN Zhao et al. (2020)	OOM	OOM	OOM	0.054 \pm 0.024	0.128 \pm 0.049	0.088 \pm 0.038
<i>Baselines with ROLAND incremental training</i>						
EvolveGCN-H Pareja et al. (2020)	0.251 \pm 0.079	0.165 \pm 0.026	0.102 \pm 0.010	0.057 \pm 0.012	0.076 \pm 0.022	0.054 \pm 0.015
EvolveGCN-O Pareja et al. (2020)	0.163 \pm 0.002	0.047 \pm 0.004	0.033 \pm 0.001	0.066 \pm 0.012	0.032 \pm 0.004	0.034 \pm 0.002
GCRN-GRU Seo et al. (2018)	0.344 \pm 0.001	0.338 \pm 0.006	0.217 \pm 0.004	0.089 \pm 0.004	0.173 \pm 0.003	0.140 \pm 0.004
GCRN-LSTM Seo et al. (2018)	0.341 \pm 0.001	0.344 \pm 0.005	0.216 \pm 0.000	0.091 \pm 0.010	0.174 \pm 0.004	0.146 \pm 0.005
GCRN-Baseline Seo et al. (2018)	0.336 \pm 0.002	0.351 \pm 0.001	0.218 \pm 0.002	0.095 \pm 0.008	0.183 \pm 0.002	0.145 \pm 0.003
T-GCN Zhao et al. (2020)	0.343 \pm 0.002	0.391 \pm 0.004	0.251 \pm 0.001	0.080 \pm 0.015	0.083 \pm 0.011	0.069 \pm 0.013
<i>ROLAND variants, topology-augmented meta-learning, and SiST-GNN</i>						
ROLAND Moving-Avg. You et al. (2022)	0.309 \pm 0.011	0.362 \pm 0.007	0.289 \pm 0.038	0.075 \pm 0.006	0.120 \pm 0.002	0.096 \pm 0.010
ROLAND MLP-Update You et al. (2022)	0.329 \pm 0.021	0.395 \pm 0.006	0.291 \pm 0.008	0.103 \pm 0.010	0.154 \pm 0.010	0.148 \pm 0.012
ROLAND GRU-Update You et al. (2022)	0.340 \pm 0.001	0.425 \pm 0.015	0.362 \pm 0.002	0.112 \pm 0.008	0.194 \pm 0.004	0.157 \pm 0.007
TMetaNet Li et al. (2025)	0.347 \pm 0.030	0.427 \pm 0.010	0.349 \pm 0.010	0.109 \pm 0.009	0.180 \pm 0.012	0.176 \pm 0.005
SiST-GNN (ours)	0.599 \pm 0.000	0.720 \pm 0.002	0.694 \pm 0.020	0.328 \pm 0.001	0.551 \pm 0.025	0.519 \pm 0.024
Improvement	+74.6%	+68.6%	+91.7%	+192.8%	+184.0%	+194.8%

Table 5: Fixed-split MRR (mean \pm std. over 5 seeds). Best per column in **bold**.

	Bitcoin-OTC	Bitcoin-Alpha	UCI-Message
GCN Kipf & Welling (2017)	0.0025	0.0031	0.1141
DynGEM Goyal et al. (2018)	0.0921	0.1287	0.1055
dyngraph2vecAE Goyal et al. (2020)	0.0916	0.1478	0.0540
dyngraph2vecAERNN Goyal et al. (2020)	0.1268	0.1945	0.0713
EvolveGCN-H Pareja et al. (2020)	0.0690	0.1104	0.0899
EvolveGCN-O Pareja et al. (2020)	0.0968	0.1185	0.1379
ROLAND Moving-Avg. You et al. (2022)	0.047 \pm 0.002	0.140 \pm 0.011	0.065 \pm 0.005
ROLAND MLP You et al. (2022)	0.078 \pm 0.002	0.156 \pm 0.011	0.088 \pm 0.011
ROLAND GRU You et al. (2022)	0.220 \pm 0.017	0.289 \pm 0.012	0.229 \pm 0.062
SiST-GNN (ours)	0.830 \pm 0.009	0.773 \pm 0.008	0.480 \pm 0.011
Improvement	+277.2%	+167.4%	+109.6%

+194.8% on Bitcoin-Alpha. The gain is consistent across different graph regimes - dense trust networks (Bitcoin), sparse messaging (UCI), large hyperlink graphs (Reddit), and long-horizon evolving topologies (AS-733), suggesting that the improvement is a property of the architecture rather than a specific dataset’s structure.

BPTT-trained baselines (EvolveGCN, GCRN, T-GCN) fail with OOM on AS-733 and Reddit benchmarks. SiST-GNN, trained under ROLAND’s incremental scheme, runs on all six datasets on a single GPU. Memory growth is constant in T because hidden states are detached between snapshots, and the augmented graph at snapshot t adds only $|\mathcal{E}_t| + N$ extra edges.

5.5 Node Classification Results

Table 6 summarises the results on the node classification task. SiST-GNN achieves the best AUC on every dataset, even though the table includes the CTDG-based model family that operates on the *native* continuous-time event stream while SiST-GNN sees only the discretized snapshot sequence.

Table 6: Dynamic node classification test AUC (%), mean \pm std for SiST-GNN over 25 random seeds). Baselines are grouped by temporal graph type: CTDG-based models and DTDG-based models. Best per column in **bold**.

	Wikipedia	Reddit	MOOC
<i>CTDG based models</i>			
JODIE Kumar et al. (2019)	80.21	63.92	60.99
TGN Rossi et al. (2020)	86.85	68.21	53.86
DyREP Trivedi et al. (2019)	83.57	53.10	65.61
TGAT da Xu et al. (2020)	85.71	67.24	63.11
APAN Wang et al. (2021b)	87.01	55.90	64.12
<i>DTDG based models</i>			
EvolveGCN-H Pareja et al. (2020)	69.81	59.27	67.92
EvolveGCN-O Pareja et al. (2020)	79.20	59.64	67.82
ROLAND You et al. (2022)	58.86 \pm 10.30	48.25 \pm 9.57	49.93 \pm 6.74
TGN Rossi et al. (2020)	50.61 \pm 13.60	49.54 \pm 6.23	50.33 \pm 4.47
TREND Wen & Fang (2022)	69.92 \pm 9.27	64.85 \pm 4.71	66.79 \pm 5.44
GraphMixer Cong et al. (2023)	65.43 \pm 4.21	60.21 \pm 5.36	63.72 \pm 4.98
SiST-GNN (ours)	84.76 \pm 3.05	72.27 \pm 1.88	83.32 \pm 0.29
Improvement (DTDG)	+7.21%	+11.41%	+22.68%

CTDG architectures (JODIE, TGN, DyREP, TGAT, APAN) consume the event ordering directly and are expected to be hard to match on a continuous-time benchmark. Yet SiST-GNN, fed only a snapshot sequence with $\Delta = 6$ h buckets, achieves comparable results to CTDG models on every dataset. Closing the CTDG–DTDG gap without any continuous-time machinery is the strongest single piece of evidence that the simultaneous-fusion construction, not the temporal interface, drives the improvement.

Restricted to the discrete-time competitors, SiST-GNN improves test AUC by +7.21% on Wikipedia (over EvolveGCN-O), +11.4% on Reddit (over TREND), and +22.8% points on MOOC (over EvolveGCN-H), a relative gain of 7 – 22%. The Wikipedia margin is particularly noteworthy because every DTDG baseline collapses to 58–79% on this dataset, suggesting that the snapshot interface alone is not the bottleneck; the bottleneck is the strict spatial/temporal ordering that SiST-GNN removes.

5.6 Ablations and Sensitivity

Sensitivity to hidden dimension. We sweep $d_h \in \{32, 64, 128, 256\}$ in Figure 2(a) and Figure 3(b). The optimal hidden dimension is dataset-dependent and does not coincide across the two tasks. On the Bitcoin trust graphs, the model peaks at $d_h = 64$ and degrades further at $d_h = 256$, consistent with overfitting on these small, sparse graphs. UCI-Message shows the opposite trend: MRR climbs monotonically from 0.266 at $d_h = 32$ to 0.334 at $d_h = 256$ and saturates past 128. The node-classification sweep is similarly heterogeneous; Wikipedia favors $d_h = 128$, Reddit is best at the smallest setting, and MOOC is essentially flat across the sweep. We set $d_h = 128$ as a single common configuration in Table 5, 4, and 6, but note that per-dataset tuning would yield small additional gains on the trust networks and Reddit.

Sensitivity to depth. We vary $L \in \{1, 2, 3, 4\}$ in Figure 2(b). A single layer is markedly weaker on every benchmark, which is expected: on the temporally augmented graph, one hop cannot reach a neighbor’s temporal counterpart *and* a second-hop neighbor. Performance rises through $L = 3$ on all three datasets, and the fourth layer is essentially neutral. We see no evidence of over-smoothing in this range: the curves *saturate* rather than decline. We default to $L = 2$ in Table 5, 4, but $L = 3$ gives a consistent 2–5 point gain when the budget allows.

GNN-backbone robustness. Figure 2(c) and Figure 3(a). On link prediction, GraphSAGE Hamilton et al. (2017) is the most consistent backbone on the Bitcoin networks, but is sharply worse on UCI-Message. The picture inverts on node classification: GCNConv dominates Reddit and MOOC, while GAT Veličković et al. (2018) is best on Wikipedia. The augmented-graph construction is therefore agnostic to the specific aggregator.

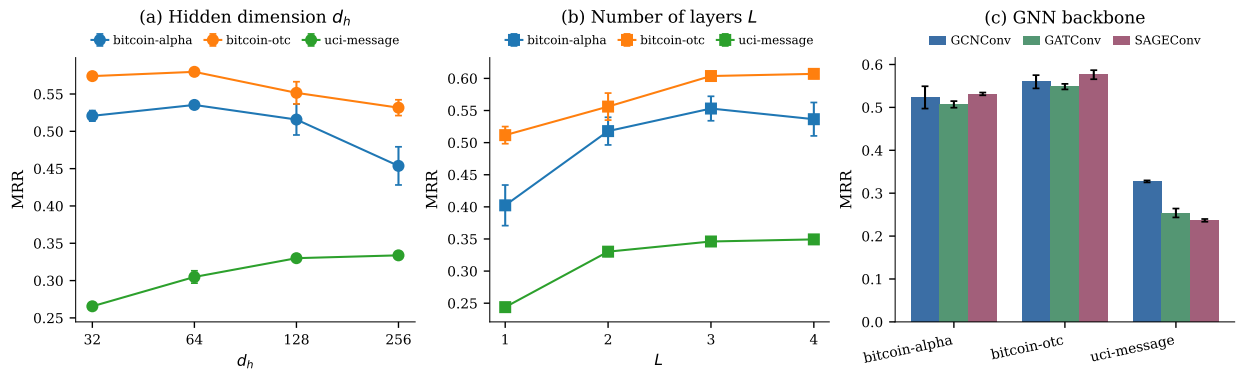


Figure 2: Sensitivity and architectural ablations on the three fixed-split datasets. **(a)** MRR vs. hidden dimension $d_h \in \{32, 64, 128, 256\}$; $d_h = 128$ sits at the Pareto knee on every benchmark. **(b)** MRR vs. number of stacked layers $L \in \{1, 2, 3, 4\}$; $L = 3$ is best on every dataset, with $L > 3$ over-smoothing on the smaller benchmarks. **(c)** Swapping the spatial backbone (GCN / GAT / SAGE) preserves the qualitative ordering, confirming that the architectural gain is a property of the temporally augmented graph rather than of any particular spatial operator. Bars and markers show the mean over 5 seeds.

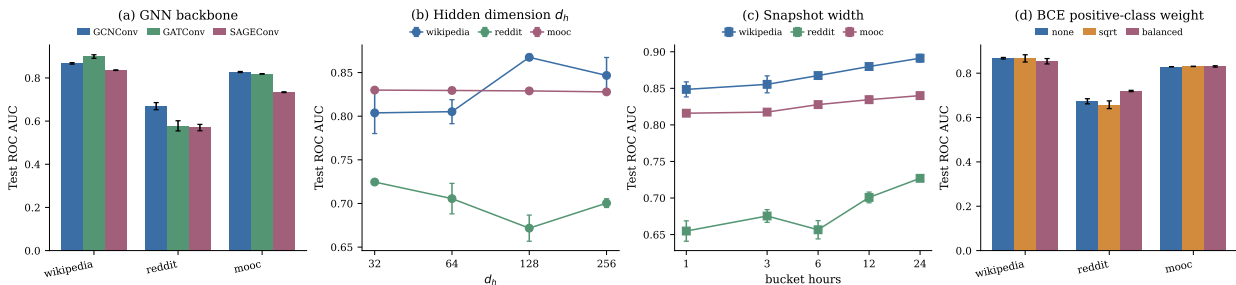


Figure 3: Sensitivity ablations for dynamic node classification (Wikipedia, Reddit, MOOC). **(a)** Spatial backbone (GCN / SAGE / GAT). **(b)** Hidden dimension $d_h \in \{32, 64, 128, 256\}$. **(c)** AUC vs. snapshot width $\Delta \in \{1, 3, 6, 12, 24\}$ h. **(d)** Positive-class weighting strategy: *none* (plain BCE), *sqrt*, *balanced*. Markers/bars are the mean of 25 seeds; error bars are one standard deviation.

Snapshot width Δ and class weighting. Figure 3(c) sweeps the discretisation width $\Delta \in \{1, 3, 6, 12, 24\}$ h. AUC rises *monotonically* with Δ on all three benchmarks. The Reddit effect is consistent with its very low positive rate (0.04%): wider buckets concentrate more rare positive events into each snapshot, giving the LSTM a less noisy temporal signal and the GNN a denser graph to aggregate over. Figure 3(d) is the complementary view through class weighting. Wikipedia and MOOC are insensitive to the BCE positive-class weight (within ± 0.015 AUC across *none*, *sqrt*, *balanced*), whereas Reddit gains +4.6 points moving from unweighted (0.673) to balanced (0.720). Discretization and reweighting are thus two complementary handles for severe class imbalance.

6 Analysis and Discussion

The sequential paradigms create an information bottleneck: a spatial-first model cannot condition its message-passing aggregator on temporal context, since none has been computed yet; a temporal-first model cannot condition its recurrent cell on the current neighborhood, since none has been observed yet. SiST-GNN dissolves this bottleneck. Consider a node u with neighbors v_1, v_2 : suppose v_1 has been consistently active (rich temporal signal, perhaps noisy current features) while v_2 has just appeared in the graph (clean current features, no history). A spatial-first model must use the structural representation of both before any temporal feature is seen; a temporal-first model must summarise both temporally before aggregation. SiST-GNN exposes the GNN to v_1 's history *and* v_2 's current features

on the same layer, letting the aggregation weights pick the right blend per-neighbor. This is the benefit of the doubled message pool discussed in Proposition 4.1, and the source of the strict generalization result of Theorem 4.1.

In datasets such as UCI-Message (+192.8%), Bitcoin-OTC (+184.0%), and Bitcoin-Alpha (+194.8%), exhibit the strongest improvements under live-update, consistent with the hypothesis that trust propagation benefits most from jointly observing a neighbor’s current rating and their historical trustworthiness trajectory. Reddit-Title’s smaller gain (+68.6%) is consistent with the relatively short temporal horizon of subreddit interaction patterns: the most predictive signal is already in the current snapshot. AS-733’s +74.6% comes despite a very long sequence, suggesting that the node recurrent state does not saturate on this horizon.

We observe that the gap between SiST-GNN and ROLAND-GRU is largest when (i) the graph has many recurring edges, so a neighbor’s recent history is highly predictive of future interactions (trust networks), and (ii) the per-snapshot node feature is uninformative on its own, so the model must rely on *either* structural neighborhood *or* temporal trajectory at any given step. When neither condition holds—e.g. on graphs whose per-snapshot features already encode a strong predictive signal—the cross-time edges contribute little additional information, and the gain shrinks, but never reverses: the extra messages can be down-weighted by the message-passing operator, but they are never adversarial.

Discretization of CTDG into buckets discards the within-bucket event order and, as the Δ -sweep in Figure 3(c) shows, the chosen Δ has a measurable effect, indicating that fine-grained discretization actually *hurts* when the positive rate is extreme because each bucket then contains too few positive events for the supervised signal. A complementary fix is to reweight the BCE loss, the **balanced** setting recovers most of the gap at fixed Δ (Figure 3(d)). Beyond discretization, a recent line of work pre-trains a dynamic-GNN encoder on auxiliary tasks and then adapts it with node- and time-conditional prompts Yu et al. (2025). Because that family relies on an upstream pre-training phase, head-to-head numbers are not directly comparable to our supervised pipeline. Designing a pre-training protocol for SiST-GNN and benchmarking it against prompt-tuned baselines on the same downstream task is a future direction. Beyond link prediction and node classification, our architecture has not yet been evaluated on dynamic benchmarks such as TGB Huang et al. (2023), on multi-task regimes, or on graph-level prediction.

7 Conclusion

We identified a structural limitation shared by virtually all snapshot-based dynamic GNNs, the strict ordering between spatial and temporal computation, and showed that fusing the two modalities *within* a single message-passing step is effective. The proposed SiST-GNN architecture doubles the per-layer distinguishable message pool, generalizes both the spatial-first and the temporal-first paradigm via two-layer composition, is permutation-equivariant, and incurs only a constant-factor overhead in per-snapshot compute. Empirically, SiST-GNN gets state-of-the-art results on the nine standard public dynamic link prediction benchmarks, with relative MRR gains of 109 – 277% (fixed-split) and 68 – 194% (live-update) over the prior method. The same architecture also transfers to dynamic node classification. SiST-GNN improves the discrete-time baseline and achieves results comparable to continuous-time baselines despite the snapshot-discretization handicap. Beyond the empirical gains, instantiating the two views of a node as neighbors in a temporally augmented graph is a general construction that may be useful wherever a model must combine evolving and structural information in a single representation. Several directions remain open. First, the current augmentation materializes a cross-time edge for every node in consecutive snapshots, and learning a sparse mask over these cross-time edges would allow the construction to scale to TGB-size graphs Huang et al. (2023). Second, extending the construction to continuous-time event streams natively would remove the snapshot-discretization step required for the JODIE node-classification benchmarks and recover the fine-grained event ordering that the binning procedure discards, which we showed to be a measurable source of error when the positive rate is extreme. Third, although the present evaluation centers on dynamic link prediction and dynamic node classification, the temporally augmented graph is task-agnostic, and applying SiST-GNN to multi-task regimes and to graph-level prediction is a natural next step. Finally, designing a pre-training protocol for SiST-GNN and benchmarking it against prompt-tuned baselines Yu et al. (2025) under a unified downstream protocol would close the remaining methodological gap with the recent pre-training and prompt-tuning line of work.

References

Weilin Cong, Si Zhang, Jian Kang, Baichuan Yuan, Hao Wu, Xin Zhou, Hanghang Tong, and Mehrdad Mahdavi. Do we really need complicated model architectures for temporal networks? In *The Eleventh International Conference on Learning Representations*, 2023. URL <https://openreview.net/forum?id=ayPPc0SyLv1>.

-
- da Xu, chuanwei ruan, evren korpeoglu, sushant kumar, and kannan achan. Inductive representation learning on temporal graphs. In *International Conference on Learning Representations*, 2020. URL <https://openreview.net/forum?id=rJeWlyHYwH>.
- ZhengZhao Feng, Rui Wang, TianXing Wang, Mingli Song, Sai Wu, and Shuibing He. A comprehensive survey of dynamic graph neural networks: Models, frameworks, benchmarks, experiments and challenges. *IEEE Transactions on Knowledge and Data Engineering*, 38(1):26–46, 2026. doi: 10.1109/TKDE.2025.3621291.
- Matthias Fey and Jan Eric Lenssen. Fast graph representation learning with pytorch geometric. *CoRR*, abs/1903.02428, 2019. URL <http://arxiv.org/abs/1903.02428>.
- Palash Goyal, Nitin Kamra, Xinran He, and Yan Liu. Dyngem: Deep embedding method for dynamic graphs. *arXiv preprint arXiv:1805.11273*, 2018.
- Palash Goyal, Sujit Rokka Chhetri, and Arquimedes Canedo. dyngraph2vec: Capturing network dynamics using dynamic graph representation learning. *Knowledge-Based Systems*, 187:104816, 2020. ISSN 0950-7051. doi: <https://doi.org/10.1016/j.knosys.2019.06.024>. URL <https://www.sciencedirect.com/science/article/pii/S0950705119302916>.
- Ehsan Hajiramezani, Arman Hasanzadeh, Nick Duffield, Krishna Narayanan, Mingyuan Zhou, and Xiaoning Qian. *Variational graph recurrent neural networks*. Curran Associates Inc., Red Hook, NY, USA, 2019.
- William L. Hamilton, Rex Ying, and Jure Leskovec. Inductive representation learning on large graphs. In *Proceedings of the 31st International Conference on Neural Information Processing Systems, NIPS’17*, pp. 1025–1035, Red Hook, NY, USA, 2017. Curran Associates Inc. ISBN 9781510860964.
- Sepp Hochreiter and Jürgen Schmidhuber. Long short-term memory. *Neural Comput.*, 9(8):1735–1780, November 1997. ISSN 0899-7667. doi: 10.1162/neco.1997.9.8.1735. URL <https://doi.org/10.1162/neco.1997.9.8.1735>.
- Shenyang Huang, Farimah Poursafaei, Jacob Danovitch, Matthias Fey, Weihua Hu, Emanuele Rossi, Jure Leskovec, Michael M. Bronstein, Guillaume Rabusseau, and Reihaneh Rabbany. Temporal graph benchmark for machine learning on temporal graphs. In *Thirty-seventh Conference on Neural Information Processing Systems Datasets and Benchmarks Track*, 2023. URL <https://openreview.net/forum?id=qG7IkQ7IB0>.
- Seyed Mehran Kazemi, Rishab Goel, Kshitij Jain, Ivan Kobyzev, Akshay Sethi, Peter Forsyth, and Pascal Poupart. Representation learning for dynamic graphs: a survey. *J. Mach. Learn. Res.*, 21(1), January 2020. ISSN 1532-4435.
- Diederik P. Kingma and Jimmy Ba. Adam: A method for stochastic optimization. In *International Conference on Learning Representations (ICLR)*, 2015. URL <https://arxiv.org/abs/1412.6980>.
- Thomas N. Kipf and Max Welling. Semi-supervised classification with graph convolutional networks. In *International Conference on Learning Representations*, 2017. URL <https://openreview.net/forum?id=SJU4ayYgl>.
- Srijan Kumar, Francesca Spezzano, V. S. Subrahmanian, and Christos Faloutsos. Edge weight prediction in weighted signed networks. In *2016 IEEE 16th International Conference on Data Mining (ICDM)*, pp. 221–230, 2016. doi: 10.1109/ICDM.2016.0033.
- Srijan Kumar, William L. Hamilton, Jure Leskovec, and Dan Jurafsky. Community interaction and conflict on the web. In *Proceedings of the 2018 World Wide Web Conference, WWW ’18*, pp. 933–943, Republic and Canton of Geneva, CHE, 2018. International World Wide Web Conferences Steering Committee. ISBN 9781450356398. doi: 10.1145/3178876.3186141. URL <https://doi.org/10.1145/3178876.3186141>.
- Srijan Kumar, Xikun Zhang, and Jure Leskovec. Predicting dynamic embedding trajectory in temporal interaction networks. In *Proceedings of the 25th ACM SIGKDD International Conference on Knowledge Discovery & Data Mining, KDD ’19*, pp. 1269–1278, New York, NY, USA, 2019. Association for Computing Machinery. ISBN 9781450362016. doi: 10.1145/3292500.3330895. URL <https://doi.org/10.1145/3292500.3330895>.
- Jure Leskovec, Jon Kleinberg, and Christos Faloutsos. Graphs over time: densification laws, shrinking diameters and possible explanations. In *Proceedings of the Eleventh ACM SIGKDD International Conference on Knowledge Discovery in Data Mining, KDD ’05*, pp. 177–187, New York, NY, USA, 2005. Association for Computing Machinery. ISBN 159593135X. doi: 10.1145/1081870.1081893. URL <https://doi.org/10.1145/1081870.1081893>.

-
- Hao Li, Hao Wan, Yuzhou Chen, Dongsheng Ye, Yulia Gel, and Hao Jiang. TMetanet: Topological meta-learning framework for dynamic link prediction. In *Forty-second International Conference on Machine Learning*, 2025. URL <https://openreview.net/forum?id=A6RjIi20NN>.
- Giang Hoang Nguyen, John Boaz Lee, Ryan A. Rossi, Nesreen K. Ahmed, Eunye Koh, and Sungchul Kim. Continuous-time dynamic network embeddings. In *Companion Proceedings of the The Web Conference 2018, WWW '18*, pp. 969–976, Republic and Canton of Geneva, CHE, 2018. International World Wide Web Conferences Steering Committee. ISBN 9781450356404. doi: 10.1145/3184558.3191526. URL <https://doi.org/10.1145/3184558.3191526>.
- Pietro Panzarasa, Tore Opsahl, and Kathleen M. Carley. Patterns and dynamics of users’ behavior and interaction: Network analysis of an online community. *Journal of the American Society for Information Science and Technology*, 60(5):911–932, 2009. doi: <https://doi.org/10.1002/asi.21015>. URL <https://onlinelibrary.wiley.com/doi/abs/10.1002/asi.21015>.
- Aldo Pareja, Giacomo Domeniconi, Jie Chen, Tengfei Ma, Toyotaro Suzumura, Hiroki Kanezashi, Tim Kaler, Tao B. Schardl, and Charles E. Leiserson. EvolveGCN: Evolving graph convolutional networks for dynamic graphs. In *Proceedings of the Thirty-Fourth AAAI Conference on Artificial Intelligence*, 2020.
- Adam Paszke, Sam Gross, Francisco Massa, Adam Lerer, James Bradbury, Gregory Chanan, Trevor Killeen, Zeming Lin, Natalia Gimelshein, Luca Antiga, Alban Desmaison, Andreas Köpf, Edward Yang, Zach DeVito, Martin Raison, Alykhan Tejani, Sasank Chilamkurthy, Benoit Steiner, Lu Fang, Junjie Bai, and Soumith Chintala. *PyTorch: an imperative style, high-performance deep learning library*. Curran Associates Inc., Red Hook, NY, USA, 2019.
- Farimah Poursafaei, Shenyang Huang, Kellin Pelrine, and Reihaneh Rabbany. Towards better evaluation for dynamic link prediction. In *Proceedings of the 36th International Conference on Neural Information Processing Systems, NIPS '22*, Red Hook, NY, USA, 2022. Curran Associates Inc. ISBN 9781713871088.
- Emanuele Rossi, Ben Chamberlain, Fabrizio Frasca, Davide Eynard, Federico Monti, and Michael Bronstein. Temporal graph networks for deep learning on dynamic graphs. In *ICML 2020 Workshop on Graph Representation Learning*, 2020.
- Aravind Sankar, Yanhong Wu, Liang Gou, Wei Zhang, and Hao Yang. Dysat: Deep neural representation learning on dynamic graphs via self-attention networks. In *Proceedings of the 13th International Conference on Web Search and Data Mining*, pp. 519–527, 2020.
- Youngjoo Seo, Michaël Defferrard, Pierre Vandergheynst, and Xavier Bresson. Structured sequence modeling with graph convolutional recurrent networks. In *Neural Information Processing: 25th International Conference, ICONIP 2018, Siem Reap, Cambodia, December 13-16, 2018, Proceedings, Part I*, pp. 362–373, Berlin, Heidelberg, 2018. Springer-Verlag. ISBN 978-3-030-04166-3. doi: 10.1007/978-3-030-04167-0_33. URL https://doi.org/10.1007/978-3-030-04167-0_33.
- Rakshit Trivedi, Mehrdad Farajtabar, Prasenjeet Biswal, and Hongyuan Zha. Dyrep: Learning representations over dynamic graphs. In *International Conference on Learning Representations*, 2019. URL <https://openreview.net/forum?id=HyePrhR5KX>.
- Petar Veličković, Guillem Cucurull, Arantxa Casanova, Adriana Romero, Pietro Liò, and Yoshua Bengio. Graph attention networks. In *International Conference on Learning Representations*, 2018. URL <https://openreview.net/forum?id=rJXmpikCZ>.
- Lu Wang, Xiaofu Chang, Shuang Li, Yunfei Chu, Hui Li, Wei Zhang, Xiaofeng He, Le Song, Jingren Zhou, and Hongxia Yang. Tcl: Transformer-based dynamic graph modelling via contrastive learning. *arXiv preprint arXiv:2105.07944*, 2021a.
- Xuhong Wang, Ding Lyu, Mengjian Li, Yang Xia, Qi Yang, Xinwen Wang, Xinguang Wang, Ping Cui, Yupu Yang, Bowen Sun, and Zhenyu Guo. Apan: Asynchronous propagation attention network for real-time temporal graph embedding. In *Proceedings of the 2021 International Conference on Management of Data, SIGMOD '21*, pp. 2628–2638, New York, NY, USA, 2021b. Association for Computing Machinery. ISBN 9781450383431. doi: 10.1145/3448016.3457564. URL <https://doi.org/10.1145/3448016.3457564>.
- Yanbang Wang, Yen-Yu Chang, Yunyu Liu, Jure Leskovec, and Pan Li. Inductive representation learning in temporal networks via causal anonymous walks. In *International Conference on Learning Representations*, 2021c. URL <https://openreview.net/forum?id=KYPz4YsCPj>.

-
- Zhihao Wen and Yuan Fang. Trend: Temporal event and node dynamics for graph representation learning. In *Proceedings of the ACM Web Conference 2022*, WWW '22, pp. 1159–1169, New York, NY, USA, 2022. Association for Computing Machinery. ISBN 9781450390965. doi: 10.1145/3485447.3512164. URL <https://doi.org/10.1145/3485447.3512164>.
- Ronald J. Williams and Jing Peng. An efficient gradient-based algorithm for on-line training of recurrent network trajectories. *Neural Comput.*, 2(4):490–501, December 1990. ISSN 0899-7667. doi: 10.1162/neco.1990.2.4.490. URL <https://doi.org/10.1162/neco.1990.2.4.490>.
- Keyulu Xu, Weihua Hu, Jure Leskovec, and Stefanie Jegelka. How powerful are graph neural networks? In *International Conference on Learning Representations*, 2019. URL <https://openreview.net/forum?id=ryGs6iA5Km>.
- Jiaxuan You, Tianyu Du, and Jure Leskovec. Roland: Graph learning framework for dynamic graphs. In *Proceedings of the 28th ACM SIGKDD Conference on Knowledge Discovery and Data Mining*, KDD '22, pp. 2358–2366, New York, NY, USA, 2022. Association for Computing Machinery. ISBN 9781450393850. doi: 10.1145/3534678.3539300. URL <https://doi.org/10.1145/3534678.3539300>.
- Le Yu, Leilei Sun, Bowen Du, and Weifeng Lv. Towards better dynamic graph learning: New architecture and unified library. In *Thirty-seventh Conference on Neural Information Processing Systems*, 2023. URL <https://openreview.net/forum?id=xHNzWHbklj>.
- Xingtong Yu, Zhenghao Liu, Xinming Zhang, and Yuan Fang. Node-time conditional prompt learning in dynamic graphs. In *The Thirteenth International Conference on Learning Representations*, 2025. URL <https://openreview.net/forum?id=kV1fYvIqaK>.
- Ling Zhao, Yujiao Song, Chao Zhang, Yu Liu, Pu Wang, Tao Lin, Min Deng, and Haifeng Li. T-gcn: A temporal graph convolutional network for traffic prediction. *IEEE Transactions on Intelligent Transportation Systems*, 21(9):3848–3858, 2020. doi: 10.1109/TITS.2019.2935152.
- Yanping Zheng, Zhewei Wei, and Jiajun Liu. Decoupled graph neural networks for large dynamic graphs. *Proc. VLDB Endow.*, 16(9):2239–2247, May 2023. ISSN 2150-8097. doi: 10.14778/3598581.3598595. URL <https://doi.org/10.14778/3598581.3598595>.
- Yifan Zhu, Fangpeng Cong, Dan Zhang, Wenwen Gong, Qika Lin, Wenzheng Feng, Yuxiao Dong, and Jie Tang. Wingnn: Dynamic graph neural networks with random gradient aggregation window. In *Proceedings of the 29th ACM SIGKDD Conference on Knowledge Discovery and Data Mining*, KDD '23, pp. 3650–3662, New York, NY, USA, 2023. Association for Computing Machinery. ISBN 9798400701030. doi: 10.1145/3580305.3599551. URL <https://doi.org/10.1145/3580305.3599551>.